

Novel gallium(III) complexes transported by *MDR1* P-glycoprotein: potential PET imaging agents for probing P-glycoprotein-mediated transport activity *in vivo*

V Sharma¹, A Beatty², S-P Wey³, J Dahlheimer¹, CM Pica¹, CL Crankshaw¹, L Bass¹, MA Green³, MJ Welch¹ and D Piwnica-Worms¹

Background: Multidrug resistance (MDR) mediated by expression of *MDR1* P-glycoprotein (Pgp) represents one of the best characterized barriers to chemotherapy in cancer patients. Positron emission tomography (PET) agents for analysis of Pgp-mediated drug transport activity *in vivo* would enable noninvasive assessment of chemotherapeutic regimens and MDR gene therapy.

Results: Candidate Schiff-base phenolic gallium(III) complexes were synthesized from their heptadentate precursors and gallium(III)acetylacetonate. Crystal structures demonstrated a hexacoordinated central gallium with overall *trans*-pseudo-octahedral geometry. Radiolabeled ⁶⁷Ga-complexes were obtained in high purity and screened in drug-sensitive (Pgp⁻) and MDR (Pgp⁺) tumor cells. Compared with control, lead compound **6** demonstrated antagonist-reversible 55-fold lower accumulation in Pgp-expressing MDR cells. Furthermore, compared with wild-type control, quantitative pharmacokinetic analysis showed markedly increased penetration and retention of **6** in brain and liver tissues of *mdr1a/b*^(-/-) gene disrupted mice, correctly mapping Pgp-mediated transport activity at the capillary blood-brain barrier and hepatocellular biliary canalicular surface *in vivo*.

Addresses: ¹Department of Molecular Biology and Pharmacology and Mallinckrodt Institute of Radiology, Washington University Medical School, St. Louis, MO 63110, USA., ²Department of Chemistry, Kansas State University, Manhattan, KS 66506, USA. ³Department of Medicinal Chemistry and Molecular Pharmacology, Purdue University, West Lafayette, IN 47907, USA.

Correspondence: David Piwnica-Worms
E-mail: piwnica-wormsd@mir.wustl.edu

Key words: gallium complexes, molecular imaging, multidrug resistance, P-glycoprotein, positron emission tomography

Received: 22 September 1999
Revisions requested: 19 October 1999
Revisions received: 14 January 2000
Accepted: 15 February 2000

Published: 19 April 2000

metadata, citation and similar papers at core.ac.uk

MDR1 Pgp as an avid transport substrate, thereby providing a useful scaffold to generate ⁶⁸Ga radiopharmaceuticals for molecular imaging of Pgp transport activity in tumors and tissues *in vivo* using PET.

© 2000 Elsevier Science Ltd. All rights reserved.

Introduction

Resistance of malignant tumors to chemotherapeutic agents is a major cause of treatment failure in patients with cancer [1,2]. One resistance phenotype, known as multidrug resistance (MDR), is characterized by the failure to respond to a variety of structurally and functionally diverse natural product cytotoxic and xenobiotic agents. *MDR1* P-glycoprotein (Pgp), a 140–180 kDa plasma membrane transporter [3,4], is one of the best characterized mediators of multidrug resistance and is reported to alter the membrane permeability to cytotoxic compounds and/or enhance the efflux of these agents out of cancer cells [1,2]. Identification *a priori* of the molecular target of a given therapeutic regimen, such as Pgp, is becoming increasingly common to select patients most likely to benefit from a given therapy. In addition, transgenic expression of the *MDR1* gene has been explored for hematopoietic cell protection in the context of cancer chemotherapy [5–7] wherein Pgp could protect hematopoietic progenitor cells from chemotherapy-induced myelotoxicity. Indeed, hematopoietic cells transduced via retroviral-mediated

transfer of the *MDR1* gene have shown preferential survival after treatment of the animal with MDR drugs [7]. Methods to interrogate Pgp transport activity have therefore been sought [8]. In this regard, various single photon emission computed tomography (SPECT) radiopharmaceuticals exemplified by ^{99m}Tc-Sestamibi [9], ^{99m}TcQ-58 [10], ^{99m}Tc-Tetrofosmin [11–13] and ^{99m}Tc-Furifosmin [12,14] have been validated as transport substrates for *MDR1* Pgp, enabling noninvasive imaging of Pgp-mediated transport activity *in vivo*. To exploit the greater sensitivity and quantification capabilities of positron emission tomography (PET), however, radiopharmaceuticals of short half-life isotopes are desired. Based on structures of known MDR cytotoxic drugs or classic modulators, several ¹¹C-labeled PET agents [15–17] or potentially ¹¹C-labeled compounds [18,19] targeting Pgp have been reported. Although promising preliminary data have been generated, the agents suffer from modest radiochemical yields and complex pharmacokinetics *in vivo* mediated, at least in part, by rapid metabolism of the radiolabeled compounds.

We sought an alternative strategy focused on discovering a non-metabolized Pgp-targeted PET agent. Schiff-base ligands [20–22] and amine phenol ligands [23,24] possessing an N_4O_2 donor core are well known. Gallium(III) complexes of selected Schiff-base ligands show potential as positron-emitting radiopharmaceuticals for use in myocardial perfusion imaging [25–28]. In addition, various stable Ga(III) complexes of this class of Schiff-base phenolic ligands also possess cytotoxic activity against tumor cells which is modified by expression of *MDR1* Pgp [29], suggesting that the compounds might be recognized as transport substrates of Pgp. Here we report the synthesis, characterization, and crystal structures of the two most favorable Pgp-targeted Ga(III) complexes, (bis(3-ethoxy-

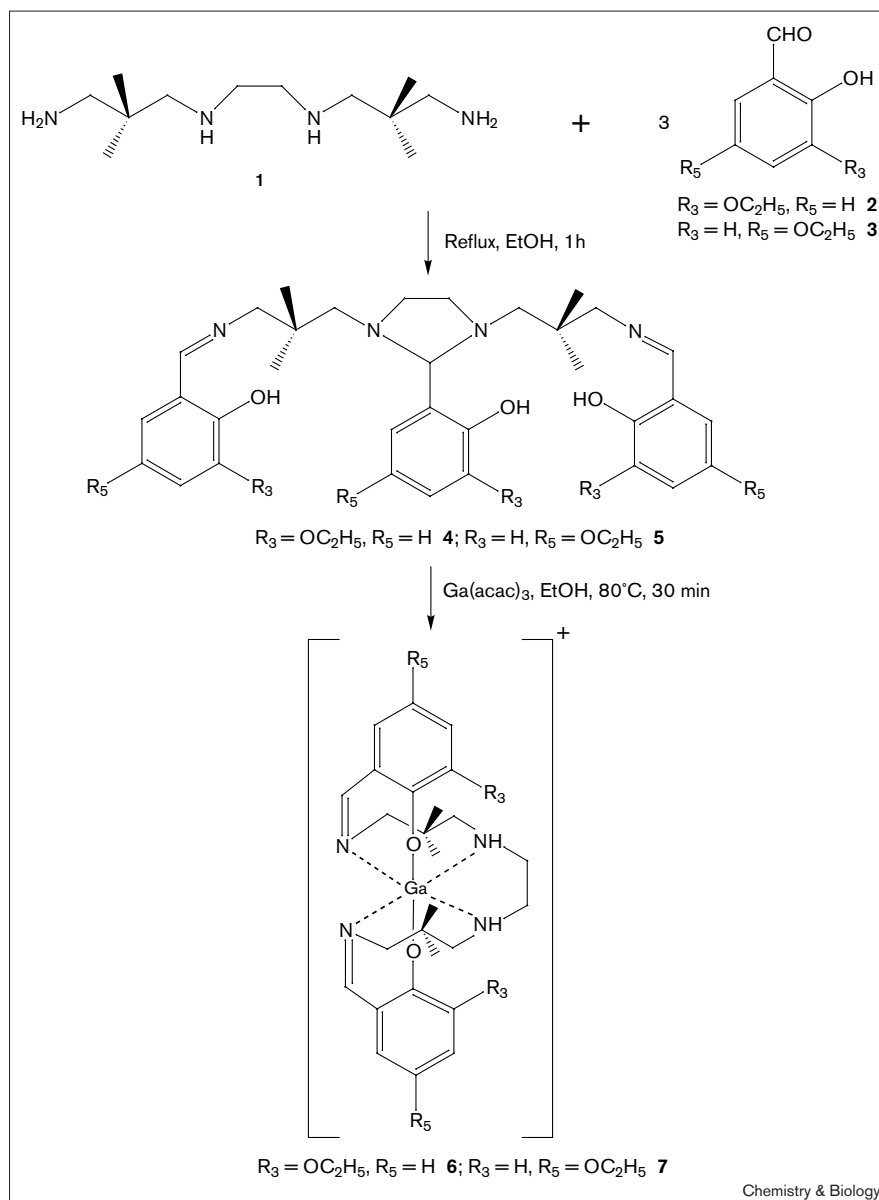
2-hydroxy-benzylidene)-*N,N'*-bis(2,2-dimethyl-3-aminopropyl)ethylenediamine)-gallium(III) perchlorate (**6**) and (bis(5-ethoxy-2-hydroxy-benzylidene)-*N,N'*-bis(2,2-dimethyl-3-aminopropyl)ethylenediamine)-gallium(III) iodide (**7**), along with tumor cell transport profiles and murine biodistributions indicating the potential for PET imaging of *MDR1* Pgp-mediated transport activity *in vivo*.

Results and discussion

Chemistry

Compounds **6** and **7** were synthesized as shown in Figure 1. Bis(*N,N'*-amino-2,2-dimethylpropane)ethylenediamine **1** was obtained by reacting dibromoethane and 2,2-dimethylpropane-1,3-diamine at room temperature.

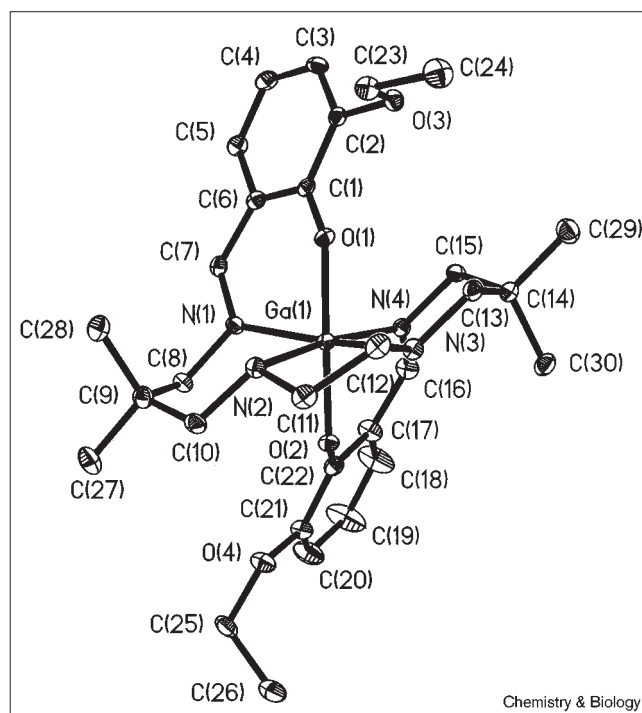
Figure 1



2-Hydroxy-3-ethoxy-benzaldehyde (**2**) was commercially available. However, 2-hydroxy-5-ethoxy-benzaldehyde (**3**) was obtained through a reaction involving 4-ethoxyphenol and paraformaldehyde using 10–20% tin(IV) chloride and triethylamine in toluene [30]. The heptadentate precursors H₃3-Eabi (**4**; 2-(2-hydroxy-3-ethoxyphenyl)-1,3-bis[4-aza-5-(2'-hydroxy-3'-ethoxyphenyl)2'',2''''-dimethyl-but-4'-ene-1'-yl]-1,3-imidazolidine) and H₃5-Eabi (**5**; 2-(2-hydroxy-5-ethoxyphenyl)-1,3-bis[4-aza-5-(2'-hydroxy-5'-ethoxyphenyl)2'',2''''-dimethyl-but-4'-ene-1'-yl]-1,3-imidazolidine). were obtained through condensation of compounds **2** or **3** and **1** in appropriate molar ratios using procedures described previously (Figure 1) [27,29]. The presence of resonance signals at 3.78 and 3.70 ppm in the ¹H NMR spectra and 91.3 and 91.8 ppm in the proton decoupled ¹³C NMR of **4** and **5**, assigned to benzylic protons and carbons, respectively, suggested formation of the expected five-membered imidazolidine rings. Furthermore, proton decoupled ¹³C NMR of **4** and **5** recorded in CDCl₃ at room temperature demonstrated 24 resonance signals supporting formation of the desired precursors. On treatment of precursors **4** and **5** with gallium(III)acetylacetonate in ethanol, cleavage of the imidazolidine ring took place leading to formation of metal complexes. The aldimino protons were shifted downfield compared with the precursors and appeared at 8.19 and 8.14 ppm in **6** and **7**, respectively, suggesting the coordination of the imine with the central gallium atom. Furthermore, the appearance of slightly broad singlets assigned to amine protons at 4.90 and 4.82 ppm in **6** and **7**, respectively, were indicative of cleavage of the imidazolidine ring, thereby providing secondary amine nitrogens for coordination with the central metal core. Furthermore, although the cleaved precursors yield achiral and flexible free ligands, these ligands form rigid complexes upon coordination with Ga(III) (Figure 1), as evident from the series of multiplets in the hydrocarbon region. We ascribe these multiplets to chirality of the coordinated amine nitrogens. Furthermore, the chemical shifts of aldimino and amine protons, including a series of overlapping signals resulting from the hydrocarbon backbone, are in accord with earlier reported gallium complexes [26,27,29]. The presence of a single set of signals due to aromatic rings and aldimino protons in ¹H NMR spectra combined with 15 resonance signals in ¹³C NMR spectra for **6** and **7** suggest the structure is symmetrical in solution [29].

Crystals suitable for X-ray crystallography were grown by slow diffusion of ether in methanol over 3–4 days and slow evaporation of methanol at room temperature for **6** and **7**, respectively. The Oak Ridge Thermal Ellipsoid Plot (ORTEP) drawings of **6** and **7** are shown in Figures 2 and 3, respectively, along with selected bond angles and interatomic distances. The crystal structure provided direct evidence that gallium is coordinated symmetrically and simultaneously to the N₄O₂ donor core of the ligand. The structure revealed that the central gallium is

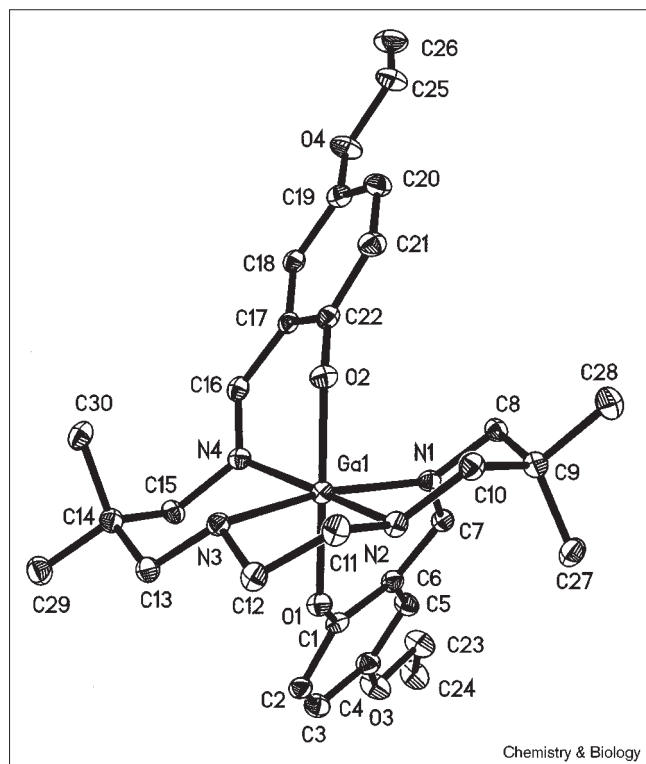
Figure 2



ORTEP drawing of [(3-ethoxy-ENBDMPI)Ga]⁺ (**6**) cation in [(3-ethoxy-ENBDMPI)Ga]ClO₄ showing the crystallographic numbering scheme. Atoms are represented by thermal ellipsoids corresponding to 20% probability. Structural parameters: pale yellow crystal, monoclinic, P2₁/c; a = 8.700(3) Å, b = 17.396(2) Å, c = 22.750(2) Å, β = 93.39(2)°; V = 3437.2(13) Å³; Z = 4; R₁ [I > 2σ(I)] = 0.0413; GOF = 1.058. Selected bond angles and interatomic distances: bond angles (deg), N1-Ga-N2, 86.73 (12); N2-Ga-N3, 84.08 (12); N3-Ga-N4, 87.90 (12); N4-Ga-N1, 101.85 (12); O1-Ga-O2, 179.02 (11); N1-Ga-N3, 168.13 (12); N2-Ga-N4, 170.52 (12); O1-Ga-N1, 87.26 (11); O1-Ga-N4, 91.87 (11); O2-Ga-N2, 87.75 (11); O2-Ga-N3, 93.45 (11); C1-O1-Ga, 125.6 (2); C22-O2-Ga, 124.1 (2); distances (Å), Ga-O1, 1.933(2); Ga-O2, 1.923 (2); Ga-N1, 2.056 (3); Ga-N2, 2.091 (3); Ga-N3, 2.104 (3); Ga-N4, 2.053 (3); O1-C1, 1.318 (4); O2-C22, 1.322 (4).

hexacoordinated involving two phenoxy oxygens (O1 and O2), two secondary amine nitrogens (N2 and N3) and two imine nitrogens (N1 and N4) with overall *trans*-pseudo-octahedral geometry. Compared with the closest gallium(III) structural analog [27], the interatomic distances of the Ga-O or Ga-N involved in the coordination sphere are similar and suggest comparable stability of the complexes. In addition, radio-thin layer chromatography (TLC) analysis of ⁶⁷Ga-labeled complexes **6** and **7** stored in saline:ethanol (90:10) for up to four days demonstrated only parent compound, further documenting stability of the complexes under aqueous conditions. As with the previously reported gallium(III) complex [27], *trans* angles involving O(1)-Ga-O(2) are close to linear. However, *trans* angles involving nitrogens exemplified by N(4)-Ga-N(2) and N(3)-Ga-N(1) (Figure 2) are 170.5(1)° and 168.1(1)°, respectively, and are ~2° more acute than the previously published gallium(III) complex. Similarly, *cis* angles involving O-Ga-N are in close

Figure 3



ORTEP drawing of [(5-ethoxy-ENBDMP)Ga]⁺ (**7**) cation in [(5-ethoxy-ENBDMP)Ga] showing the crystallographic numbering scheme. Atoms are represented by thermal ellipsoids corresponding to 20% probability. Structural parameters: pale yellow crystal, monoclinic, P2₁/c; a = 8.0987(8) Å, b = 20.394(2) Å, c = 20.603(2) Å; β = 95.239(8)°; V = 3388.7(6) Å³; Z = 4; R₁ [I > 2σ(I)] = 0.0333; GOF = 1.136. Selected bond angles and interatomic distances: bond angles (deg), N1-Ga-N2, 87.07 (13); N2-Ga-N3, 83.26 (13); N3-Ga-N4, 87.65 (13); N4-Ga-N1, 102.43 (13); O1-Ga-O2, 178.89(12); N1-Ga-N3, 168.58 (13); N2-Ga-N4, 169.84 (13); O1-Ga-N1, 87.20 (12); O1-Ga-N4, 91.54 (12); O2-Ga-N2, 88.56 (13); O2-Ga-N3, 92.86 (12); C1-O1-Ga, 123.4 (3); C22-O2-Ga, 122.0 (2); distances (Å), Ga-O1, 1.926 (3); Ga-O2, 1.924(3); Ga-N1, 2.066 (3); Ga-N2, 2.089 (3); Ga-N3, 2.126 (3); Ga-N4, 2.066 (3); O1-C1, 1.330 (5); O2-C22, 1.333 (5).

agreement to values observed previously [27,31], suggesting a mildly distorted octahedral geometry around the gallium. The smallest angle N2-Ga-N3 can be attributed to the restrictions of the five-membered chelate ring involving N(2), C(11), C(12), N(3) and Ga. In comparison with the 3-ethoxy substituted compound **6** (Figure 2), the 5-ethoxy analog **7** (Figure 3) was highly similar in its distances and angles around the coordination sphere. However, C1-O1-Ga and C22-O2-Ga are 123.4(3)° and 122.0(2)°, respectively, and are 2° more acute in **7** compared to **6**, suggesting slight variation in the positions of the peripheral constituents of each molecule, including the aromatic rings.

Cell transport assays

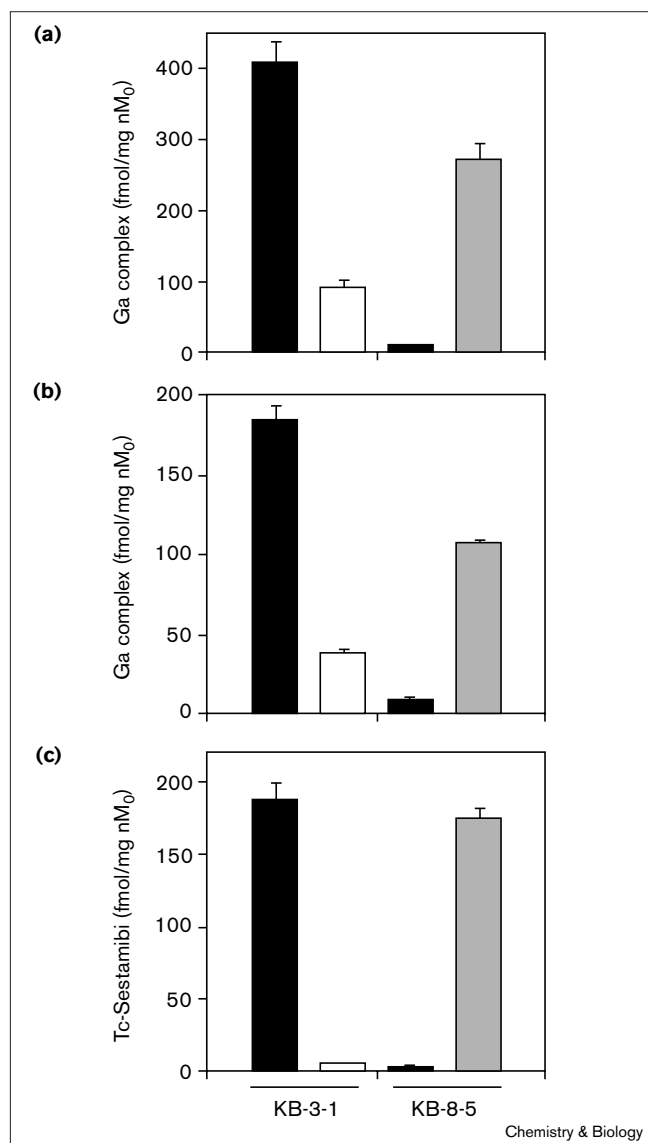
Radiolabeled ⁶⁷Ga complexes were obtained via ⁶⁷Ga(acetylacetonate)₃ and precursors **4** and **5** in ethanol at 80°C for

30 min using published procedures [27]. Final reaction mixtures were passed through nylon syringe filters (0.2 μm) and silica to remove excess ligand. Synthesis and workup could be accomplished in less than an hour, an interval of significant practical value for potential PET radiopharmaceuticals labeled with ⁶⁸Ga (t_{1/2} = 68 min), which is obtained from commercially available ⁶⁸Ge (t_{1/2} = 271d) generators. Compounds were assessed for their radiopharmaceutical purity by radio-TLC [methanol:saline, 90:10; R_f:0.47(**6**), 0.48(**7**)] and found to be > 95% pure.

⁶⁷Ga(III) complexes were evaluated for their *MDR1* Pgp-mediated transport activity in a whole-cell transport assay using drug-sensitive human epidermal carcinoma KB-3-1 cells and the colchicine-selected *MDR* derivative KB-8-5 cells as described previously [12,32]. KB-3-1 cells do not express Pgp, whereas KB-8-5 cells express modest levels of Pgp as documented by Western blot analysis with mAb C219 [10]. Net cell content of many hydrophobic cationic tracers transported by Pgp is a function of both passive potential-dependent influx and transporter-mediated efflux [33]. Accordingly, favorable cationic ⁶⁷Ga complexes should highly penetrate KB-3-1 cells as result of the inwardly directed electrochemical driving forces [32]. As a further test of membrane potential-dependent influx, incubation of KB-3-1 cells in 120 mM K⁺/20 mM Cl⁻ buffer containing the potassium ionophore valinomycin (1 μg/ml) has been shown to collapse mitochondrial and plasma membrane-potentials toward zero, and reduce net tracer uptake of membrane potential-responsive hydrophobic cations [9,34]. Net accumulation of the ⁶⁷Ga complexes should, therefore, be reduced in high K⁺/valinomycin buffer, and furthermore, tracer levels greater than that expected from equilibrium distribution into the water spaces under these conditions provide one measure of nonspecific adsorption to hydrophobic compartments within the cells [9]. Conversely, *MDR1*-Pgp-mediated outward transport of candidate ⁶⁷Ga complexes would be expected to decrease net cellular accumulation in KB-8-5 cells compared with KB-3-1 cells. In addition, the potent *MDR1* Pgp antagonist GF120918 [33,35] should enhance tracer accumulation in KB-8-5 cells by inhibiting the outward transport function of Pgp. Desirable *MDR1* targeted complexes would therefore have the following properties: low nonspecific binding to membranes and hydrophobic compartments of cells; high distinction in net uptake levels between drug-sensitive cells and *MDR* cells; and significant enhancement of uptake in *MDR* cells upon addition of an *MDR* antagonist [12].

In drug-sensitive KB-3-1 cells, the 3-ethoxy-substituted ⁶⁷Ga-complex **6** demonstrated plateau accumulation of 410 ± 28 fmol (mg protein)⁻¹ (nM₀)⁻¹ (n = 4), 55-fold greater than drug-resistant KB-8-5 cells (Figure 4a). This was similar to the 48-fold difference (Figure 4c) observed

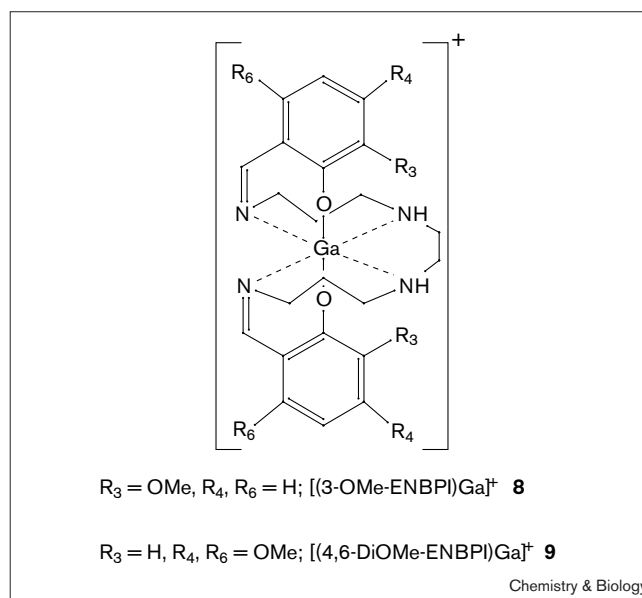
Figure 4



Characterization of (a) [(3-ethoxy-ENBDMPi)⁶⁷Ga]⁺ (6), (b) [(5-ethoxy-ENBDMPi)⁶⁷Ga]⁺ (7) and (c) ^{99m}Tc-Sestamibi accumulation in KB-3-1 cells (left-hand columns) and MDR KB-8-5 cells (right-hand columns) as indicated. Shown is net uptake at 30 min [fmol/(mg protein·nM₀)] using control buffer (black bars), 130 mM K⁺/valinomycin buffer (open bars), and control buffer containing the MDR modulator GF120918 (300 nM; gray bars). Each bar represents the mean of four determinations; line above the bar denotes ± SEM.

with ^{99m}Tc-Sestamibi (Cardiolite™, hexakis(2-methoxyisobutylisocyanide)technetium(I) chloride), a previously validated agent tested under identical conditions [12], and indicated that 6 was an avid transport substrate recognized by human MDR1 Pgp. In KB-3-1 cells, accumulation of 6 was 4.5-fold greater in control buffer than in the presence of high K⁺/valinomycin buffer, consistent with a significant response to depolarization of membrane potential. The final cell accumulation value was 91.2 ± 7.9 fmol (mg

Figure 5



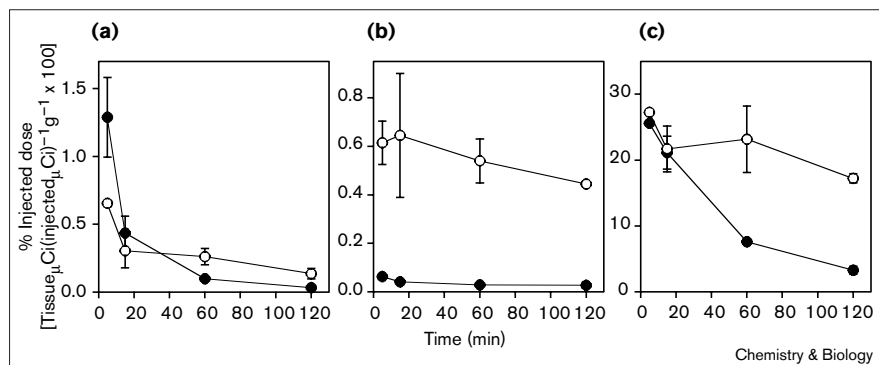
Structures of [(3-methoxy-ENBPI)⁶⁷Ga]⁺ (8) and [(4,6-dimethoxy-ENBPI)⁶⁷Ga]⁺ (9).

protein)⁻¹ (nM₀)⁻¹ (n = 4), greater than the value expected based on the cell water space estimated for these cells (5.4 μl/mg protein [12]) implying a significant level of non-specific adsorption of the complex to hydrophobic components within the cells. Addition of GF120918 at a concentration known to maximally inhibit Pgp (300 nM [10]) enhanced cellular accumulation of 6 in MDR cells towards that observed in drug-sensitive cells, again consistent with a favorable transport profile.

Using the same techniques, we also radiolabeled the 3-methoxy analog 8 and the 4,6-dimethoxy analog 9 of the non-substituted hydrocarbon backbone ligands (Figure 5) [29]. In comparison to 6, the drug-sensitive/drug-resistant cell uptake ratios were significantly less for these Ga(III) complexes (30 min cell uptake [fmol (mg protein)⁻¹ (nM₀)⁻¹] in KB-3-1 cells, in KB-8-5 cells, and KB-3-1/KB-8-5 ratio: 8, 47 ± 5, 17 ± 1, 2.8; 9, 252 ± 20, 42 ± 2, 6.0). Thus the methyl substitutions in the hydrocarbon backbone coupled with the ethoxy functionality of 6 significantly improved the transport profile of the complex.

Variation in the position of the ethoxy group to the 5 position on the aromatic ring resulted in a less robust Pgp-mediated transport profile, however (Figure 4b). The 5-ethoxy-substituted ⁶⁷Ga-complex 7 showed only a 23-fold greater accumulation in drug-sensitive KB-3-1 cells compared with KB-8-5 cells, and furthermore, addition of GF120918 to drug-resistant KB-8-5 cells enhanced accumulation of 7 to a lesser degree. Of note, 7 showed a similar response as 6 to high K⁺/valinomycin buffer, suggesting a

Figure 6



Pharmacokinetics of [(3-ethoxy-ENBDMP)]⁶⁷Ga⁺ (**6**) in (a) blood, (b) brain and (c) liver of FVB mice. Wild-type (●) and *mdr1a/1b*^(-/-) mice (○) were administered **6** by bolus injection into a lateral tail vein and organs harvested at the indicated times for analysis. Data are expressed as percent of injected dose of radioactivity per gram tissue at each respective time point. Data points represent the mean of 2–4 determinations each; error bars represent ± SEM when larger than the symbol.

similar level of lipid partitioning. The greater octanol/water partitioning coefficient for the 3-ethoxy analog **6**, for example, compared with Tc-Sestamibi ($\log P = 1.7$ versus $\log P = 1.1$, respectively), would be consistent with the enhanced potential-independent cell accumulation (membrane absorption) seen with the ⁶⁷Ga complexes.

Biodistribution studies in *mdr1a/1b*^(-/-) mice

To demonstrate the potential use of radiolabeled Ga complexes as imaging markers of Pgp-mediated transport *in vivo*, we performed quantitative pharmacokinetic analysis in mice following intravenous injection of the tracer. Mice have two isoforms of Pgp (*mdr1a* and *mdr1b*) which confer multidrug resistance [36]. The drug-transporting *mdr1a* Pgp isoform is expressed in capillary endothelial cells of the brain wherein the protein is a major component of the blood–brain barrier [37]. Here, Pgp limits entry of a variety of amphipathic compounds into the central nervous system [36]. Drug-transporting Pgp isoforms are also expressed along the biliary cannalicular surface of hepatocytes wherein the transporters function to secrete substrates into the bile [36]. In this regard, *mdr1a/1b*^(-/-) gene-disrupted mice, which have no drug-transporting Pgp, are a robust model for evaluation of candidate MDR agents by interrogating net tracer accumulation into brain and liver tissues [10].

Thus, we analyzed initial tissue uptake and retention of ⁶⁷Ga-complex **6** in *mdr1a/1b*^(-/-) mice in comparison to wild-type FVB mice (Figure 6). Relative to wild-type mice, *mdr1a/1b*^(-/-) mice showed tenfold more ⁶⁷Ga-complex **6** in brain parenchyma 5 minutes after injection of the complex (Figure 6b). Additionally, the area under the curve from 5–120 minutes (AUC_{5-120}) of **6** in *mdr1a/1b*^(-/-) brain was $62.5 \pm 16.1 \mu\text{Ci (injected } \mu\text{Ci)}^{-1} (\text{g tissue})^{-1} \times 100 \times \text{min}$ ($n = 8$), a value 17-fold greater than wild-type mice ($p < 0.005$). By contrast, blood retention of **6** in *mdr1a/1b*^(-/-) mice was $29.4 \pm 8.7 \mu\text{Ci (injected } \mu\text{Ci)}^{-1} (\text{g tissue})^{-1} \times 100 \times \text{min}$, only 1.2-fold that of wild-type control ($p > 0.5$; Figure 6a). Because blood flow to the brain does not differ between *mdr1* gene disrupted and

wild-type mice [38], the marked enhancement in initial penetration and retention of **6** in brain tissue of *mdr1a/1b*^(-/-) mice cannot be attributed to differences in cerebral perfusion. Pilot imaging experiments using planar scintigraphy also demonstrated increased visualization of ⁶⁷Ga-complex **6** in the brains of *mdr1a/1b*^(-/-) mice, compared to control (data not shown), thus showing promise for eventual quantitative imaging by clinical or microPET [39]. Furthermore, **6** shows 3–5-fold greater differences in brain AUC_{5-120} between wild-type and *mdr1*^(-/-) mice than ^{99m}Tc-Sestamibi [40], ^{99m}TcQ-58 [10] and ^{99m}Tc-Tetrofosmin [13], further documenting its potential superiority for imaging Pgp activity *in vivo*.

In liver, initial accumulation of **6** was comparable between *mdr1a/1b*^(-/-) and wild-type mice (Figure 6c). However, liver clearance was markedly delayed in *mdr1a/1b*^(-/-) mice consistent with blockade of Pgp-mediated biliary secretion of the tracer. The AUC_{5-120} of **6** in liver tissue of *mdr1a/1b*^(-/-) mice was $2465 \pm 440 \mu\text{Ci (injected } \mu\text{Ci)}^{-1} (\text{g tissue})^{-1} \times 100 \times \text{min}$, twofold greater than wild-type mice. These data further validate ⁶⁷Ga-complex **6** as a substrate for Pgp *in vivo* and show its potential as a molecular imaging probe of transporter function and inhibition in the living organism.

Significance

One of the best characterized barriers to chemotherapy in cancer patients is multidrug resistance (MDR) mediated by expression of the *MDR1* P-glycoprotein (Pgp). We wanted to develop agents for use in positron emission tomography (PET) to allow noninvasive assessment of chemotherapy regimens and MDR gene therapy. Selected Schiff-base phenolic complexes of Ga(III) are shown to be probes of *MDR1* Pgp-mediated transport activity. Variation in the position of the ethoxy group from *para* to *ortho* with respect to the Ga-O-C bond increased *MDR1* Pgp recognition *in vitro*, suggesting that the unique *MDR1* Pgp transport properties of the 3-ethoxy Ga(III)-complex **6** lie in the spatial orienta-

tion of the peripheral constituents of the molecule rather than within the inner coordination sphere. Biodistribution analysis demonstrated that differences in Pgp transport activity could be readily detected with tracer concentrations of ^{67}Ga -labeled **6** in *mdr1a/1b*^(-/-) gene-disrupted mice compared to control, and, therefore, ^{68}Ga analogs of **6** may provide useful scaffolds to generate a PET radiopharmaceutical for quantifying the functional status of Pgp in tumors and tissues *in vivo*.

Materials and methods

General methods

1,2-dibromoethane, 2,2-dimethylpropane-1,3-diamine, 3-ethoxysalicylaldehyde and **2** were obtained from Aldrich Chemical Co. Ga(III)acetylacetonate was purchased from Mathey-Johnson/Alfa Chemical Co. ^1H and ^{13}C NMR spectra were recorded on a VARIAN 300 MHz spectrometer; chemical shifts are reported in δ (ppm) with reference to TMS. Mass spectra were obtained from the Washington University Resource for Biomedical and Bioorganic Mass Spectrometry with 3-nitrobenzyl alcohol as a matrix. Molar conductance (κ , $\Omega^{-1}\text{mol}^{-1}\text{cm}^2$) was determined with a portable conductivity meter (Orion Research, model 120) at 25°C in acetonitrile with 0.37 mM solutions of each complex. Octanol/water partition coefficients (*P*) were determined with radiolabeled compounds using standard methods. Elemental analyses (C, H, N) were performed by Galbraith Laboratories, Knoxville, TN. Synthesis of the radiolabeled compound $^{99\text{m}}\text{Tc}$ -Sestamibi was performed with a one-step kit formulation (Cardiolite™, E. I. Du Pont, Medical Products Division, Billerica, MA) [32].

Bis(*N,N'*-amino-2,2-dimethylpropane)ethylenediamine (**1**)

Potassium hydroxide (4.0 g, 71.3 mmol) was added to dibromoethane (3.0 g, 15.9 mmol) in acetonitrile (35 ml). The stirred suspension was treated with 2,2-dimethylpropane-1,3-diamine (excess) and stirred at room temperature for 24 h. Contents were filtered, filtrate evaporated and residue distilled under reduced pressure to yield colorless liquid **1** (2.73 g, 11.9 mmol, 74.3%); bp 120–125°C/0.5 mm Hg; ^1H NMR (300 MHz, CDCl_3) δ : 0.80 (s, 12H), 1.18 (bs, 6H), 2.38 (m, 4H), 2.50 (m, 4H), 2.64 (m, 4H); ^{13}C NMR (75.4 MHz, CDCl_3) δ : 23.5, 35.2, 49.7, 51.2, 58.3.

2-hydroxy-5-ethoxy-benzaldehyde (**3**)

4-Ethoxyphenol (1.28 g, 9.26 mmol) and trioctylamine (1.64 g, 4.63 mmol) dissolved in toluene (20 ml) were treated with dropwise addition of tin tetrachloride (1.85 ml, 1.0 M) and stirred for 30 min at room temperature. Paraformaldehyde (0.83 g, 27.8 mmol) was added and refluxed at 90°C for 10 h. The contents were cooled to room temperature, hydrolyzed and acidified to pH 2.5, extracted with methylene chloride (3 × 100 ml), dried over anhydrous sodium sulfate, filtered, evaporated, and the residue purified on silica using 1% ethylacetate in hexane. Further evaporation of eluent yielded colorless crystals **3** (0.90 g, 5.42 mmol, 58.5%); mp 52–53°C; ^1H NMR (300 MHz, CDCl_3) δ : 1.42 (t, 3H), 4.02 (q, 2H), 6.92 (d, 1H), 6.99 (d, 1H), 7.14 (dd, 1H), 9.84 (s, 1H), 10.65 (s, 1H); ^{13}C NMR (75.4 MHz, CDCl_3) δ : 14.6, 64.2, 116.1, 118.6, 120.1, 125.8, 152.1, 156.0, 196.4.

2-(2-hydroxy-3-ethoxyphenyl)-1,3-bis[4-aza-5-(2'-hydroxy-3'-ethoxyphenyl)2'',2'''-dimethyl-but-4'-ene-1'-yl]-1,3-imidazolidine (*H*₃3-Eabi; **4**)

Compound **4** was prepared using methods described previously [27,29]. ^1H NMR (300 MHz, CDCl_3) δ : 0.81 (s, 6H), 0.83 (s, 6H), 1.40 (t, 3H), 1.49 (t, 6H), 2.28 (d, 2H), 2.55 (d, 2H), 2.69 (m, 2H), 3.05 (d, 2H), 3.40 (d, 2H), 3.52 (d, 2H), 3.78 (s, 1H), 4.05 (q, 2H), 4.09 (q, 4H), 7.10 (m, 2H), 7.20–7.80 (m, 7H), 8.06 (s, 2H); ^{13}C NMR (75.4 MHz, CDCl_3) δ : 14.6, 14.7, 24.2, 24.4, 36.3, 54.2, 62.2, 64.1, 64.7, 67.3, 91.3, 114.7, 115.4, 117.3, 118.1, 118.4, 122.8, 123.7, 147.1, 147.8, 148.2, 152.8, 165.3, 165.4.

2-(2-hydroxy-5-ethoxyphenyl)-1,3-bis[4-aza-5-(2'-hydroxy-5'-ethoxyphenyl)2'',2'''-dimethyl-but-4'-ene-1'-yl]-1,3-imidazolidine (*H*₃5-Eabi; **5**)

Compound **5** was prepared using the methods described previously [27,29]. ^1H NMR (300 MHz, CDCl_3) δ : 0.82 (s, 6H), 0.84 (s, 6H), 1.34 (t, 3H), 1.40 (t, 6H), 2.26 (d, 2H), 2.58 (d, 2H), 2.66 (m, 2H), 3.08 (d, 2H), 3.40 (d, 2H), 3.58 (m, 2H), 3.70 (s, 1H), 3.82 (q, 2H), 4.0 (q, 4H), 6.60 (d, 1H), 6.70 (d, 2H), 6.78–7.00 (m, 6H), 8.05 (s, 2H); ^{13}C NMR (75.4 MHz, CDCl_3) δ : 14.7, 14.9, 24.4, 24.6, 36.3, 54.3, 54.6, 62.3, 64.1, 68.0, 91.8, 115.8, 116.8, 117.4, 117.7, 118.4, 119.7, 123.1, 151.1, 151.5, 154.7, 155.3, 164.9, 165.1.

[(3-ethoxy-ENBDMPI)Ga]⁺ ClO₄⁻ (**6**)

Using the procedure described previously [27,29], *H*₃3-Eabi (**4**; 0.14 g, 0.21 mmol), gallium(III)acetylacetonate (0.08 g, 0.21 mmol), and potassium perchlorate (0.03 g, 0.21 mmol) were reacted in methanol. Pale yellow needles were washed with methanol, then ether and dried to yield **6** (0.10 g, 0.14 mmol, 67.6%); mp 190–192°C dec; ^1H NMR (300 MHz, DMSO-d_6) δ : 0.90 (s, 6H), 0.95 (s, 6H), 1.40 (t, 6H), 2.60 (m, 2H), 2.70–2.98 (m, 6H), 3.60 (dd, 2H), 3.78 (t, 2H), 4.02 (q, 4H), 4.90 (bs, 2H), 6.60 (t, 2H), 6.88 (dd, 2H), 7.02 (d, 2H), 8.19 (s, 2H); ^{13}C NMR (75.4 MHz, CDCl_3) δ : 14.8, 21.9, 26.1, 35.5, 47.6, 59.0, 63.2, 68.9, 115.9, 116.2, 118.8, 125.3, 150.4, 157.2, 170.5; MS(FAB) for $[\text{C}_{30}\text{H}_{44}\text{N}_4\text{O}_4\text{Ga}]^+$ *m/z* = 594.1; κ ($\Omega^{-1}\text{mol}^{-1}\text{cm}^2$) 120; Anal. calcd. for $\text{C}_{30}\text{H}_{44}\text{N}_4\text{O}_8\text{GaCl}\cdot\text{CH}_3\text{OH}$: C, 51.29; H, 6.66; N, 7.72; found: C, 50.99; H, 6.78; N, 7.52.

[(5-ethoxy-ENBDMPI)Ga]⁺ I⁻ (**7**)

Using the procedure described previously [27,29], *H*₃5-Eabi (**5**; 59 mg, 0.09 mmol), gallium(III)acetylacetonate (0.03 g, 0.09 mmol), and potassium iodide (14 mg, 0.09 mmol) were reacted in methanol. Pale yellow needles were washed with methanol, then ether and dried to yield **7** (43 mg, 0.06 mmol, 68.6%); mp 185–188°C dec; ^1H NMR (300 MHz, DMSO-d_6) δ : 0.77 (s, 6H), 0.93 (s, 6H), 1.28 (t, 6H), 2.61–2.82 (m, 6H), 2.88 (m, 2H), 3.28 (d, 2H), 3.79 (d, 2H), 3.90 (q, 4H), 4.82 (bs, 2H), 6.81 (d, 2H), 6.83 (d, 2H), 7.05 (dd, 2H), 8.14 (s, 2H); ^{13}C NMR (75.4 MHz, CDCl_3) δ : 14.3, 21.5, 25.9, 35.1, 47.0, 59.4, 62.9, 68.9, 115.7, 117.7, 122.4, 123.9, 148.5, 160.9, 169.6; MS(FAB) for $[\text{C}_{30}\text{H}_{44}\text{N}_4\text{O}_4\text{Ga}]^+$ *m/z* = 594.1; κ ($\Omega^{-1}\text{mol}^{-1}\text{cm}^2$) 130; Anal. calcd. for $\text{C}_{30}\text{H}_{44}\text{N}_4\text{O}_4\text{GaI}\cdot\text{CH}_3\text{OH}$: C, 49.42; H, 6.42; N, 7.43; found: C, 49.09; H, 6.70; N, 7.34.

X-ray crystallography

Crystal data were collected on a single crystal of **6** (0.7 × 0.3 × 0.2 mm) obtained from slow diffusion of ethyl ether into a solution of **6** in methanol, and on a crystal of **7** (0.4 × 0.4 × 0.3 mm) obtained from slow evaporation of a methanol solution, using a Siemens P4 four-circle diffractometer with graphite monochromated Mo- K_α radiation ($\lambda = 0.71073 \text{ \AA}$) at 173 K. The experimental details and refinement procedures are separately reported in the Supplementary material section. Crystallographic tables S1–5 for **6** and **7** containing crystal data and structure refinement parameters, atomic coordinates and equivalent isotropic displacement parameters ($\text{\AA}^2 \times 10^3$), bond lengths (\AA) and angles ($^\circ$), anisotropic displacement parameters ($\text{\AA}^2 \times 10^3$), hydrogen coordinates ($\times 10^4$) and isotropic displacement parameters ($\text{\AA}^2 \times 10^3$) also are included in the Supplementary material section.

Cell transport assays

Cell culture. Monolayers of human epidermoid carcinoma KB 3-1 cells and the colchicine-selected KB 8-5 derivative cell lines were grown as described previously [9,41]. Briefly, cells were plated in 100 mm Petri dishes containing seven 25 mm glass coverslips on the bottom and grown to confluence in DMEM (GIBCO, Grand Island, NY) supplemented with L-glutamine (1%), penicillin/streptomycin (0.1%), and heat-inactivated fetal calf serum (10%) in the presence of 0 and 10 ng/ml colchicine, respectively.

Solutions and reagents. Stock solutions of GF120918 (gift of Glaxo-Wellcome, Research Triangle Park, NC) were prepared in

dimethyl sulfoxide (DMSO). Final concentration of DMSO in experimental buffers was <1%, which has been found to have no effect on net uptake of tracer complexes in cultured cells [42]. All other reagents were obtained from Sigma Chemical Co. Control solution for transport experiments was a modified Earle's balanced salt solution (MEBSS) containing: 145 mM Na⁺, 5.4 mM K⁺, 1.2 mM Ca²⁺, 0.8 mM Mg²⁺, 152 mM Cl⁻, 0.8 mM H₂PO₄⁻, 0.8 mM SO₄²⁻, 5.6 mM dextrose, 4.0 mM HEPES, and 1% bovine calf serum (vol/vol), pH 7.4 ± 0.05. A 130 mM K⁺/20 mM Cl⁻ solution was made by equimolar substitution of potassium methanesulfonate for NaCl as described previously [43].

Transport assays. Coverslips with confluent cells were used for studies of cell transport and kinetics as described previously [9]. In brief, cells were removed from culture media and washed for 15–30 s in MEBSS. Accumulation experiments were initiated by immersing coverslips in 60 mm glass Pyrex dishes containing 4 ml loading solution consisting of MEBSS with 1–6 nM [⁶⁷Ga-complex] (300–900 pmol/mCi; 1–2 μCi/ml). Coverslips with cells were removed at various times, rinsed 3 × in 25 ml ice-cold isotope-free solution for 8 s to clear extracellular spaces, and placed in 35 mm plastic Petri dishes. Cells were extracted in 1% sodium dodecylsulfate with 10 mM sodium borate before protein assay by the method of Lowry *et al.* [44] using bovine serum albumin as the protein standard. Aliquots of the loading buffer and stock solutions also were obtained for standardizing cellular data with extracellular concentration of each Ga complex. Cell extracts, stock solutions and extracellular buffer samples were assayed for gamma activity in a well-type sodium iodide gamma counter (Cobra II, Packard, Meridan, Conn.). Absolute concentration of total Ga complex in solution was determined from the activity of stock solutions and specific activity of ⁶⁷Ga. Data are reported as fmol Ga complex (mg protein)⁻¹ (nM_o)⁻¹ as previously described, with (nM_o)⁻¹ representing total concentration of Ga-complex in the extracellular buffer [45].

Biodistribution studies

Vertebrate animal procedures were approved by the appropriate institutional review committee. Distribution of ⁶⁷Ga complex in the blood, liver and brain tissues of parental strain FVB mice (FVB/NTacBR) and FVB *mdr1a/1b*^(-/-) gene knockout mice (FVB/TacBR-[KO]*mdr1a*-[KO]*mdr1b*N7) (Taconic, Germantown, NY) was determined as described previously [10,46]. ⁶⁷Ga-complex was diluted in 90:10 saline:ethanol to a final concentration of 20 μCi/ml. Mice were anesthetized by metaface inhalation and injected with 2 μCi of radiotracer via bolus injection through a tail vein. Animals were sacrificed by cervical dislocation at 5, 15, 60 and 120 min post-injection (n = 2–4 each). Blood samples were obtained by cardiac puncture and tissues harvested rapidly. Gamma activity in organ samples was counted for 1 min, or until two standard deviations of sampling were below 0.5%. Data are expressed as percent of injected dose per gram of tissue [(tissue μCi) (injected μCi)⁻¹ (g tissue)⁻¹ × 100]. From biodistribution time-activity curves, area-under-the-curve (AUC) was calculated using trapezoidal integration (KaleidaGraph, Synergy Software) and reported as tissue μCi (injected μCi)⁻¹ (g tissue)⁻¹ × 100 × min. Data are generally reported as mean ± SEM. Pairs were compared by Student's *t* test. Values of *p* ≤ 0.05 were considered significant.

Supplementary material

Supplementary material including details of crystallographic conditions is available at <http://current-biology.com/supmat/supmatin.htm>.

Acknowledgements

This work was supported by a grant from the US Department of Energy (DE-FG02-94ER61885).

References

- Gottesman, M.M. & Pastan, I. (1993). Biochemistry of multidrug resistance mediated by the multidrug transporter. *Annu. Rev. Biochem.* **62**, 385-427.
- Bosch, I. & Croop, J. (1996). P-glycoprotein multidrug resistance and cancer. *Biochim. Biophys. Acta* **1288**, F37-F54.
- Gros, P., Ben Neriah, Y., Croop, J.M. & Housman, D.E. (1986). Isolation and expression of a complementary DNA that confers multidrug resistance. *Nature* **323**, 728-731.
- Shen, D.W., *et al.*, & Gottesman, M.M. (1986). Human multidrug-resistant cell lines: increased *mdr1* expression can precede gene amplification. *Science* **232**, 643-645.
- Sorrentino, B., *et al.*, & Nienhuis, A. (1992). Selection of drug-resistant bone marrow cells *in vivo* after retroviral transfer of human MDR1. *Science* **257**, 99-103.
- Podda, S., *et al.*, & Bank, A. (1992). Transfer and expression of the human multiple drug resistance gene into live mice. *Proc. Natl Acad. Sci. USA* **89**, 9676-9680.
- Hanania, E., Fu, S., Roninson, I., Zu, Z., Gottesman, M. & Deisseroth, A. (1995). Resistance to taxol chemotherapy produced in mouse marrow cells by safety-modified retroviruses containing a human MDR-1 transcription unit. *Gene Ther.* **2**, 279.
- Homolya, L., Hollo, Z., Germann, U.A., Pastan, I., Gottesman, M.M. & Sarkadi, B. (1993). Fluorescent cellular indicators are extruded by the multidrug resistance protein. *J. Biol. Chem.* **268**, 21493-21496.
- Piwonica-Worms, D., Chiu, M., Budding, M., Kronauge, J., Kramer, R. & Croop, J. (1993) Functional imaging of multidrug-resistant P-glycoprotein with an organotechnetium complex. *Cancer Res.* **53**, 977-984.
- Luker, G., Rao, V., Crankshaw, C., Dahlheimer, J. & Piwnica-Worms, D. (1997). Characterization of phosphine complexes of technetium (III) as transport substrates of the multidrug resistance (MDR1) P-glycoprotein and functional markers of P-glycoprotein at the blood-brain barrier. *Biochemistry* **36**, 14218-14227.
- Ballinger, J.R., Bannerman, J., Boxen, I., Firby, P., Hartman, N.G. & Moore, M.J. (1996). Technetium-99m-Tetrofosmin as a substrate for P-glycoprotein: *in vitro* studies in multidrug-resistant breast tumor cells. *J. Nucl. Med.* **37**, 1578-1582.
- Crankshaw, C., *et al.*, & Piwnica-Worms, D. (1998). Novel Tc(III)-Q-complexes for functional imaging of the multidrug resistance (MDR1) P-glycoprotein. *J. Nucl. Med.* **39**, 77-86.
- Chen, W., Luker, K., Dahlheimer, J., Pica, C., Luker, G. & Piwnica-Worms, D. (2000). Effects of MDR1 and MDR3 P-glycoproteins, MRP1 and BCRP/MXR/ABCP on transport of Tc-99m-Tetrofosmin. *Biochem. Pharmacol.* in press.
- Ballinger, J., Muzzammil, T. & Moore, M. (1997). Technetium-99m-Furifosmin as an agent for functional imaging of multidrug resistance in tumors. *J. Nucl. Med.* **38**, 1915-1919.
- Elsinga, P.H., *et al.*, & Vaalburg, W. (1996). Carbon-11-labeled daunorubicin and verapamil for probing P-glycoprotein in tumors with PET. *J. Nucl. Med.* **37**, 1571-1575.
- Hendrikse, N., Franssen, E., van der Graaf, W., Vaalburg, W. & de Vries, E. (1999). Visualization of multidrug resistance *in vivo*. *Eur. J. Nucl. Med.* **26**, 283-293.
- Hendrikse, N., *et al.*, & Franssen, E. (1999). A new *in vivo* method to study P-glycoprotein transport in tumors and the blood-brain barrier. *Cancer Res.* **59**, 2411-2416.
- Mehta, B.M., Rosa, E., Fissekis, J.D., Bading, J.R., Biedler, J.L. & Larson, S.M. (1992). *In vivo* identification of tumor multidrug resistance with tritium-3-colchicine. *J. Nucl. Med.* **33**, 1373-1377.
- Mehta, B., Rosa, E., Biedler, J. & Larson, S. (1994). *In vivo* uptake of carbon-14-colchicine for identification of tumor multidrug resistance. *J. Nucl. Med.* **35**, 1179-1184.
- Isobe, T., Kida, S. & Misumi, S. (1967). Preparation of schiff base complexes of lanthanides(III) ions. *Bull. Chem. Soc. Japan* **40**, 1862-1863.
- Bailey, N.A., McKenzie, E.D. & Worthington, J.M. (1977). Molecular structure (X-ray analysis) of a dinuclear iron(III) compound formed with the [N₄O₂] ligand 'sal₂trien'. *Inorg. Chim. Acta* **25**, L137-L138.
- Evans, D.F. & Jakubovic, D.A. (1988). Water soluble hexadentate schiff-base ligands as sequestering agents for iron(III) and gallium(III). *J. Chem. Soc. Dalton Trans.* 2927-2933.
- Wong, E., Liu, S., Lugger, T., Hahn, F.E. & Orvig, C. (1995). Hexadentate N₄O₂ amine phenol complexes of gallium and indium. *Inorg. Chem.* **34**, 93-101.
- Wong, E., Caravan, P., Liu, S., Rettig, S. & Orvig, C. (1996). Selectivity of potentially hexadentate amine phenols for Ga⁺³ and In⁺³ in aqueous solution. *Inorg. Chem.* **35**, 715-724.
- Green, M.A., Welch, M. & Huffman, J. (1984). Synthesis and crystallographic characterization of a gallium salicylaldehyde complex of radiopharmaceutical interest. *J. Am. Chem. Soc.* **106**, 3689-3691.
- Tsang, B., Mathias, C. & Green, M. (1993). A gallium-68 radiopharmaceutical that is retained in myocardium: ⁶⁸Ga-[(4,6-MeO)₂sal₂BAPEN]⁺. *J. Nucl. Med.* **34**, 1127-1131.

27. Tsang, B., Mathias, C., Fanwick, P. & Green, M. (1994). Structure-distribution relationship for metal-labelled myocardial imaging agents: comparison of a series of cationic gallium(III) complexes with hexadentate bis(salicylaldehyde) ligands. *J. Med. Chem.* **37**, 4400-4406.
28. Wey, S. (1995). Synthesis, characterization, and structure-activity relationships of gallium, indium, and copper-labeled radiopharmaceuticals for myocardial imaging with PET [*Ph.D. Thesis*]. Purdue University, West Lafayette, IN.
29. Sharma, V., Crankshaw, C. & Piwnica-Worms, D. (1996). Effects of multidrug resistance (*MDR1*) P-glycoprotein expression levels and coordination metal on the cytotoxic potency of multidentate (N_4O_2) ethylenediamine-bis[propyl(R-benzylimino)]metal(III) cations. *J. Med. Chem.* **39**, 3483-3490.
30. Casiraghi, G., Casnati, G., Puglia, G., Sartori, G. & Terenghi, G. (1980). Selective reactions between phenols and formaldehyde. A novel route to salicylaldehydes. *J. Chem. Soc. Perkin. Trans. I.* 1862-1865.
31. Sharma, V., Beatty, A., Goldberg, D.E. & Piwnica-Worms, D. (1997). Structure of novel antimalarial gallium(III) complex with selectivity against chloroquine-resistant *P. falciparum*. *J. Chem. Soc. Chem. Commun.*, 2223-2224.
32. Piwnica-Worms, D., Rao, V., Kronauge, J. & Croop, J. (1995). Characterization of multidrug-resistance P-glycoprotein transport function with an organotechnetium cation. *Biochemistry* **34**, 12210-12220.
33. Sharma, V. & Piwnica-Worms, D. (1999). Metal complexes for therapy and diagnosis of drug resistance. *Chem. Rev.* **99**, 2545-2560.
34. Chernoff, D.M., Strichartz, G.R. & Piwnica-Worms, D. (1993). Membrane potential determination in large unilamellar vesicles with hexakis(2-methoxyisobutyl isonitrile) technetium(I). *Biochim. Biophys. Acta* **1147**, 262-266.
35. Hyafil, F., Vergely, C., Du Vignaud, P. & Grand-Perret, T. (1993). *In vitro* and *in vivo* reversal of multidrug resistance by GF120918, an acridonecarboxamide derivative. *Cancer Res.* **53**, 4595-4602.
36. Schinkel, A.H., Mol, C.A.A.M., Wagenaar, E., van Deemter, L., Smit, J.J.M. & Borst, P. (1995). Multidrug resistance and the role of P-glycoprotein knockout mice. *Eur. J. Cancer* **31**, 1295-1298.
37. Schinkel, A., *et al.*, & Borst, P. (1994). Disruption of the mouse *mdr1a* P-glycoprotein gene leads to a deficiency in the blood-brain barrier and to increased sensitivity to drugs. *Cell* **77**, 491-502.
38. Hendrikse, N., *et al.*, & Franssen, E. (1998). Complete *in vivo* reversal of P-glycoprotein pump function in the blood-brain barrier visualized with positron emission tomography. *Br. J. Pharmacol.* **124**, 1413-1418.
39. Cherry, S., *et al.*, & Phelps, M.M. (1997) MicroPET: a high resolution PET scanner for imaging small animals. *IEEE Trans. Nucl. Sci.* **44**, 1161-1166.
40. Dahlheimer, J., Crankshaw, C., Marmion, M. & Piwnica-Worms, D. (1997). Modulation of the pharmacokinetics of P-glycoprotein-targeted Tc-99m-complexes by GW0918 (GG918) in wild-type and *mdr1a* P-glycoprotein knock-out mice. *Proc. Am. Assoc. Cancer Res.* **38**, 590.
41. Akiyama, S.I., Fojo, A., Hanover, J.A., Pastan, I. & Gottesman, M.M. (1985). Isolation and genetic characterization of human KB cell lines resistant to multiple drugs. *Somatic Cell Mol. Genet.* **11**, 117-126.
42. Chiu, M.L., Kronauge, J.F. & Piwnica-Worms, D. (1990). Effect of mitochondrial and plasma membrane potentials on accumulation of hexakis (2-methoxyisobutyl isonitrile) technetium(I) in cultured mouse fibroblasts. *J. Nucl. Med.* **31**, 1646-1653.
43. Piwnica-Worms, D., Jacob, R., Horres, C.R. & Lieberman, M. (1983). Transmembrane chloride flux in tissue-cultured chick heart cells. *J. Gen. Physiol.* **81**, 731-748.
44. Lowry, O.H., Rosenbrough, W.F., Farr, A.L. & Randall, R.J. (1951). Protein measurements with the folin phenol reagent. *J. Biol. Chem.* **193**, 265-275.
45. Piwnica-Worms, D., Kronauge, J. & Chiu, M. (1990). Uptake and retention of hexakis (2-methoxy isobutyl isonitrile) technetium(I) in cultured chick myocardial cells: mitochondrial and plasma membrane potential dependence. *Circulation* **82**, 1826-1838.
46. Herman, L.W., Sharma, V., Kronauge, J.F., Barbarics, E., Herman, L.A. & Piwnica-Worms, D. (1995). Novel hexakis(areneisonitrile)-technetium(I) complexes as radioligands targeted to the multidrug resistance P-glycoprotein. *J. Med. Chem.* **38**, 2955-2963.